Scaling Behavior of Adsorption on Patchwise Bivariate Surfaces Revisited

F. Bulnes, A. J. Ramirez-Pastor, and G. Zgrablich*

Departamento de Física and Laboratorio de Ciencias de Superficies y Medios Porosos, Universidad Nacional de San Luis, CONICET, Chacabuco917, 5700 San Luis, Argentina

Received August 23, 2006. In Final Form: October 20, 2006

The adsorption of gases on patchwise heterogeneous bivariate surfaces is studied. These surfaces are characterized by a collection of strong and weak adsorbing patches with a typical length scale l. Different forms and spatial arrangements of these patches determine different topographies characterized by an *effective length*, $l_{\text{eff}} = \sigma l$, where σ takes values from 1 to 4 for the different topographies considered here. Previous studies showed that the mean square deviation between isotherms corresponding to different values of l_{eff} scaled as a power law with exponent α, without providing any physical interpretation of such behavior. In the present work, we introduce a different scaling function, $\chi(l)$, which is shown to be twice the difference in free energy per site between a reference isotherm and the given isotherm, at half coverage. With this function the scaling behavior and the value of the scaling exponent α are determined over the whole range of interparticles interaction energy and adsorptive energy, and for different temperatures, through Monte Carlo simulations. The results are similar to those obtained in previous studies, with a value of α which is half the one obtained before due to the different definition of the scaling function, but the present analysis provides a full understanding of the scaling behavior based on the physical significance of the scaling function and the scaling exponent.

1. Introduction

Gas−solid interactions[1] are the fundamental physical entities for the understanding of adsorption, which is the first step in a variety of processes in surface science and its applications, such as gas separation, catalysis, and thin films growth. For a given gas−solid system, the gas−solid interaction is given by an *adsorptive energy surface*,[2−4] AES, i.e., the energy surface *seen* by a particle at the distance of adsorption on the solid surface, representing the variation along the solid surface of the gas−solid interaction potential minimum. Given the gas particle and the solid, the AES can be calculated following the method described in ref 4. For the great majority of real systems the AES is not a flat, or even a periodic, surface but a quite irregular one resembling a mountainous landscape. Such a solid surface is regarded as heterogeneous, and it has been shown that heterogeneity affects strongly many molecular processes occurring at the gas−solid interface.[5−9]

In the past the adsorptive energy distribution has been considered as the only important characteristic to be known to describe the behavior of adsorbed particles, and much effort was dedicated to the development of methods for its determination from experimental adsorption data.[5,10] However, it has been shown[11−16] that many gas−solid surface processes are strongly affected, not only by the adsorptive energy distribution but also by the way these energies are spatially distributed (energetic topography). It is then a challenge in the field of gas−solid interactions to envisage methods for the determination of the energetic topography of heterogeneous substrates from adsorption experiments (characterization problem).

By looking at the AES corresponding to solids with random impurities or defects, such as those obtained in ref 4, it becomes clear that the energetic topography is spatially correlated and is far from the idealistic random site distribution, being much closer to a patchwise structure with finite size patches of stronger and weaker sites. It is therefore reasonable to attempt an approach to the characterization problem by studying very simple topographies, such as those arising in bivariate surfaces, i.e., surfaces composed of two kinds of sites, say weak and strong sites with adsorptive energies ϵ_1 and ϵ_2, respectively, arranged in patches of size l. Recent developments in the theory of adsorption on heterogeneous surfaces, such as the *supersite approach*,[16] and experimental advances in the tailoring of nanostructured adsorbates,[17,18] encourage this kind of study. Once the behavior of bivariate surfaces is fully understood and methods to extract l from adsorption experiments are developed, then one

* Corresponding author. E-mail: giorgio@unsl.edu.ar.

(1) Steele, W. A. *The Interaction of Gases with Solid Surfaces*; Pergamon Press: New York, 1974.
(2) Zgrablich, G. *Annales Universitatis Mariae Curie-Sklodowska, Vol. LIV/LV*, 17, Lublin, 2000; p 285.
(3) Zgrablich, G.; Ciacera, M.; Gargiulo V.; Sales, J. L. *Appl. Surf. Sci.* **2002**, *196*, 41.
(4) Nazzarro M.; Zgrablich, G. *Langmuir* **2003**, *19*, 6737.
(5) Jaroniec M.; Madey, R. *Physical Adsorption on Heterogeneous Surfaces*, Elsevier: Amsterdam, 1988.
(6) Rudzinski W.; Everett, D. H. *Adsorption of Gases on Heterogeneous Surfaces*; Academic Press: New York, 1992.
(7) Rudzinski, W., Steele, W. A., Zgrablich, G., Eds. *Equilibria and Dynamics of Gas Adsorption on Heterogeneous Solid Surfaces*; Elsevier: Amsterdam, 1997.
(8) Bulnes, F.; Nieto, F.; Pereyra, V.; Zgrablich G.; Uebing, C. *Langmuir* **1999**, *15*, 5990.
(9) Bulnes, F.; Pereyra, V.; Riccardo J. L.; Zgrablich, G. *J. Chem. Phys.* **1999**, *111*, 1.
(10) Jaroniec M.; Bräuer, P. *Surf. Sci. Rep.* **1986**, *6*, 65.
(11) Riccardo, J. L.; Chade, M. A.; Pereyra V. D.; Zgrablich, G. *Langmuir* **1992**, *8*, 1518.
(12) Zgrablich, G.; Mayagoitia, V.; Rojas, F.; Bulnes, F.; González, A. P.; Nazzarro, M.; Pereyra, V.; Ramírez-Pastor, A. J.; Riccardo, J. L.; Sapag, K. *Langmuir* **1996**, *12*, 129.
(13) Zgrablich, G.; Zuppa, C.; Ciacera, M.; Riccardo J. L.; Steele, W. A. *Surf. Sci.* **1996**, *356*, 257.
(14) Riccardo, J. L.; Zgrablich, G.; Steele, W. A. *Appl. Surf. Sci.* **2002**, *196*, 138.
(15) Gargiulo, M. V.; Sales, J. L.; Ciacera, M.; Zgrablich, G. *Surf. Sci.* **2002**, *501*, 282.
(16) Steele, W. A. *Langmuir* **1999**, *15*, 6083.
(17) Yang, M. X.; Gracias, D. H.; Jacobs, P. W.; Somorjai, G. *Langmuir* **1998**, *14*, 1458.
(18) Lopinski, G. P.; Wayner, D. D. M.; Wolkow, R. A. *Nature* **2000**, *406*, 48.

10.1021/la062491s CCC: $37.00
Published on Web 12/02/2006

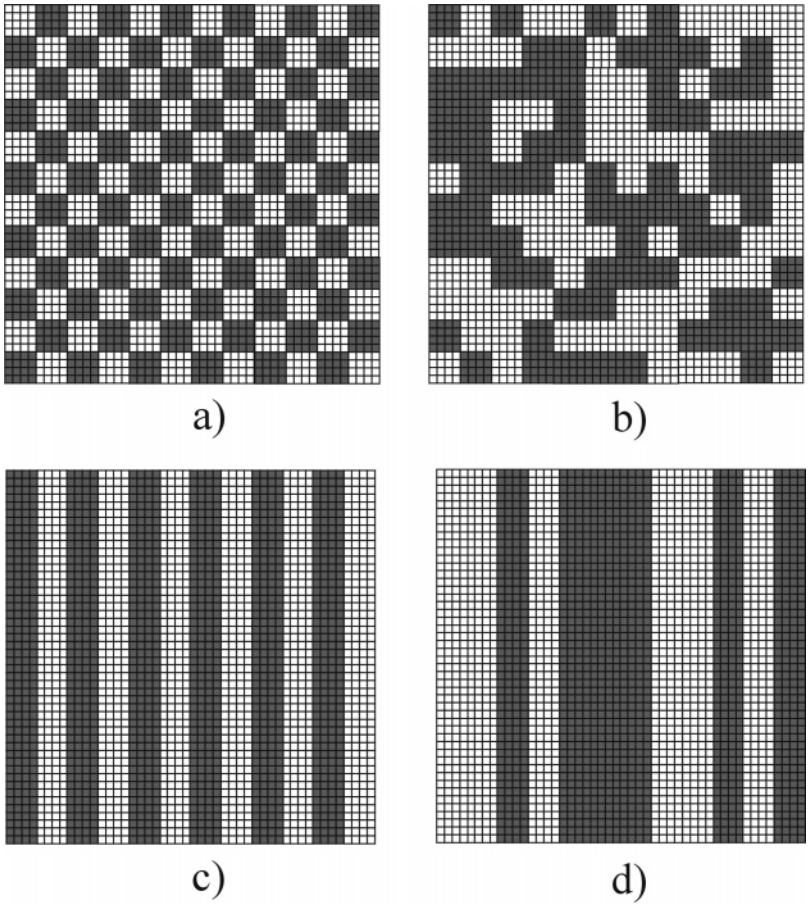

Figure 1. Schematic representation of heterogeneous bivariate surfaces with chessboard (a), random square patches (b), ordered strips (c), and random strips (d) topography. The patch size in the figure is $l = 4$.

could go over to develop the theory for multivariate surfaces, which could probably mimic satisfactorily general heterogeneous surfaces.

Adsorption on bivariate surfaces with square patches and strip topographies has recently been studied through Monte Carlo simulations for the case of particles with nearest neighbor interaction energy.[19−22] It was found that both adsorption isotherms and differential heats of adsorption follow scaling laws involving the patch size l with a universal exponent and that this characteristic length defining the topography could, in principle, be obtained from the analysis of experimental results. These scaling laws, however, appeared in a quite mysterious way without the basis of a physical interpretation. The scope of the present work is to provide such a basis for the observed scaling behavior. In section 2 we present the adsorption model and briefly review the most important simulation results obtained in previous works. These results are discussed from a new point of view in section 3, where a physical interpretation of the scaling behavior is constructed. General conclusions are given in section 4.

2. Model and Simulation Results

We assume that the substrate is represented by a two-dimensional square lattice of dimension $L \times L$ adsorption sites, with a total of M sites, with periodic boundary conditions. Each adsorption site can be either a "weak" site, with adsorptive energy ϵ_1, or a "strong" site, with adsorptive energy ϵ_2 ($\epsilon_1 < \epsilon_2$). Weak and strong sites form patches of different geometry:

(a) Square patches of size l ($l = 1, 2, 3, ...$), which are spatially distributed either in a deterministic alternate way (chessboard topography), Figure 1a, or in a non-overlapping random way (random topography), Figure 1b.

(b) Strips of transversal size l ($l = 1, 2, 3, ...$), which are spatially distributed either in an ordered alternate way, Figure 1c, or in a non-overlapping random way (random topography), Figure 1d.

To easily identify a given topography, we introduce the notation l_C for a chessboard topography of size l and, similarly, l_R for random square patches, l_{OS}, for ordered strips and l_{RS} for random strips. Then, in Figure 1a−d, the topographies are 4_C, 4_R, 4_{OS}, and 4_{RS}, respectively. We also use the notation "bp" to refer to the extreme case of big patches topography ($l \rightarrow \infty$), i.e., a surface with one-half of weak sites and one-half of strong sites.

The substrate is exposed to an ideal gas phase at temperature T and chemical potential μ. Particles can be adsorbed on the substrate with the restriction of at most one adsorbed particle per site and we consider a nearest neighbor (NN) interaction energy w among them (we use the convention $w > 0$ for repulsive and $w < 0$ for attractive interactions). Then the adsorbed phase is characterized by the Hamiltonian

$$H = -M[(\epsilon_1\theta_1 + \epsilon_2\theta_2) - \mu\theta] + w\sum_{(i,j)} n_i n_j \qquad (1)$$

(19) Bulnes, F.; Ramirez-Pastor, A. J.; Zgrablich, G. *J. Chem. Phys.* **2001**, *115*, 1513.
(20) Bulnes, F.; Ramirez-Pastor, A. J.; Zgrablich, G. *Adsorp. Sci. Technol.* **2001**, *19*, 229.
(21) Bulnes, F.; Ramirez-Pastor, A. J.; Zgrablich, G. *Phys. Rev. E* **2002**, *65*, 31603.
(22) Romá, F.; Bulnes, F.; Ramirez-Pastor, A. J.; Zgrablich, G. *Phys. Chem. Chem. Phys.* **2003**, *5*, 3694.

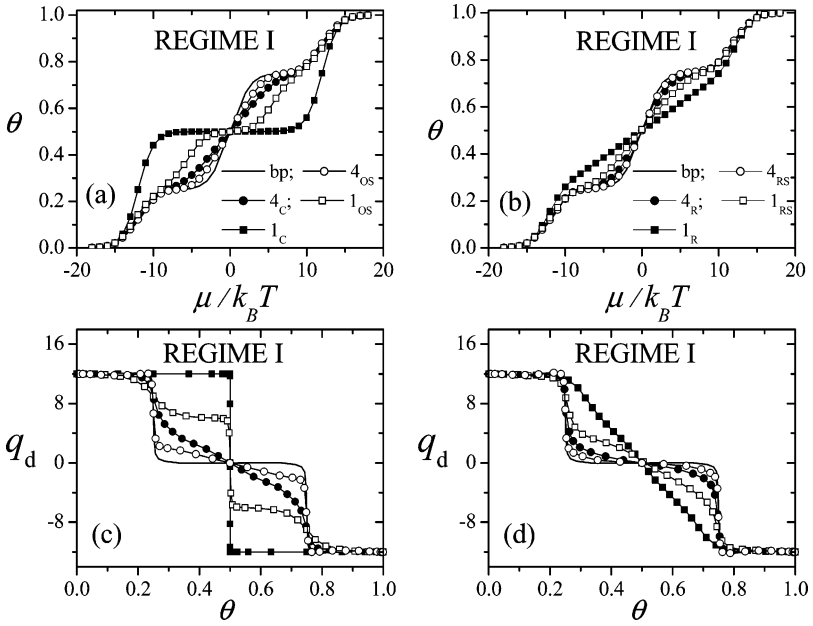

Figure 2. Adsorption isotherms (a−b) and differential heats of adsorption (c−d) for different square patch topographies corresponding to Regime I (in this case $\Delta E = 12$, $w = 3$). Symbols in (c) and (d) are as in (a) and (b), respectively.

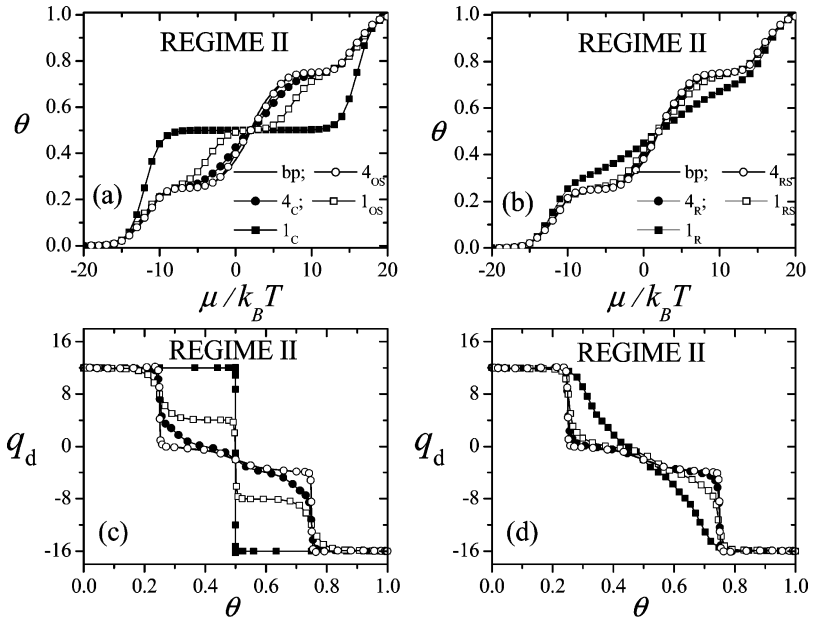

Figure 3. Adsorption isotherms (a−b) and differential heats of adsorption (c−d) for different square patch topographies corresponding to Regime II (in this case $\Delta E = 12$, $w = 4$). Symbols in (c) and (d) are as in (a) and (b), respectively.

where $\theta = \theta_1 + \theta_2$ is the total surface coverage (summing the coverages on weak and strong sites), n_i is the site occupation number (=0 if empty or =1 if occupied), and the sum runs over all pairs of NN sites (i,j). Without any loss of generality, we can consider that all energies are measured in units of k_BT (k_B being the Boltzmann constant) and that $\epsilon_1 = 0$ and $\epsilon_2 = \epsilon_1 + \Delta E$, in such a way that the adsorptive energy is characterized by the single adimensional parameter ΔE.

The adsorption process is simulated through a grand canonical ensemble Monte Carlo (GCEMC) method, following the procedure described in detail in previous works,[19−22] and mean values are obtained for the surface coverage θ and the internal energy U as

$$\theta = \langle N \rangle / M; \quad U = \langle H \rangle - \mu \langle N \rangle \tag{2}$$

where N is the number of adsorbed particles and the brackets denote averages over statistically uncorrelated configurations. From these, the differential heat of adsorption q_d as a function of the coverage is calculated as[23]

$$q_d(\theta) = \left[\frac{\partial U}{\partial \theta}\right]_T \tag{3}$$

The typical behavior of adsorption isotherm and differential heat of adsorption is shown in Figures 2 and 3 for square patches and strips topographies.

Figure 2 shows the behavior of adsorption isotherms, (a−b), and $q_d(\theta)$, (c−d), for different topographies for $w = 3$, $\Delta E =$

(23) Bakaev, V.; Steele, W. A. *Langmuir* **1992**, *8*, 148.

12, and $k_BT = 1$. It can be seen that all curves are contained between two limit ones: the one corresponding to 1_C and the one corresponding to bp. For chessboard topographies, four different adsorption processes can be visualized (they can be seen as separated by shoulders in the adsorption isotherm and by steps in q_d): (i) strong site patches are filled first up to $\theta = 0.25$, forming a $c(2 \times 2)$ structure on them (in this region $q_d = 12$); (ii) as long as $4w < \Delta E$, the filling of strong site patches is completed up to $\theta = 0.5$ (in this region q_d decreases continuously from 12, zero occupied NN, to 0, four occupied NN); processes (iii) and (iv), corresponding to the regions $0.5 < \theta < 0.75$ and $0.75 < \theta < 1$, respectively, are equivalent to processes (i) and (ii) for weak site patches. Random topographies are seen to behave in a similar way with a particularly interesting feature: the behavior of random topography of size l seems to approach that for chessboard topography with an effective size $l_{eff} > l$. As can be easily understood, as long as the condition $w/\Delta E \leq 1/4$ is satisfied, the adsorption process is similar to the one described above; i.e., strong site patches are filled first and weak site patches are filled after. We call this feature Regime I.

Figure 3 shows the behavior of adsorption isotherms, (a−b), and $q_d(\theta)$, (c−d), for different topographies for $w = 4$, $\Delta E = 12$, and $k_BT = 1$. In this case, where $w/\Delta E \geq 1/3$, the adsorption process follows a different regime, which we call Regime II: (i) the strong site patches are filled until the $c(2 \times 2)$ ordered phase is formed on them; (ii) the weak site patches are filled until the $c(2 \times 2)$ ordered phase is formed on them; (iii) the filling of the strong site patches is completed; (iv) the filling of the weak site patches is completed.

These two regimes have been visually observed in simulation snapshots (not shown here). It should be noticed that Regimes I and II are disconnected. In between, i.e., $1/4 < w/\Delta E < 1/3$, the system behaves in a mixed transition regime changing continuously from one to another.

Qualitatively similar results for adsorption isotherms and differential heat of adsorption (not shown) were obtained at other temperatures corresponding to values of k_BT ranging from 2 to 10.

3. Discussion

In previous works[19−22] the quantity

$$\chi_a = \int_{-\infty}^{+\infty} |\theta(\mu) - \theta^R(\mu)|^2 \, d\mu$$

(ref 24) inspired in a kind of "mean square deviation" was used to test the scaling behavior of adsorption, where θ^R is a reference isotherm. It was found that this quantity scaled with the patch size l as a power law with a scaling exponent α. However, no physical explanation was found for this behavior. In the present analysis we use instead the quantity

$$\chi = \int_{-\infty}^{+\infty} |\theta(\mu) - \theta^R(\mu)| \, d\mu \quad (4)$$

which, as we shall show below, is related to the difference in free energy in the processes of filling the two involved surfaces and therefore leads to a physical interpretation of the scaling behavior.

By taking as a reference isotherm the one corresponding to the bp topography, we find that, for a given adsorption regime, the functions χ collapse on a single curve for any topography when represented in terms of an *effective length scale* (representing an effective patch size), l_{eff}, given by

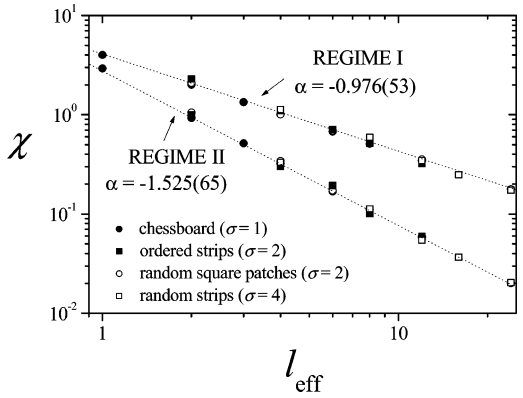

Figure 4. Power-law behavior of the function $\chi(l)$, showing the collapse of data for different topographies on a single curve for each adsorption regime when the effective length scale l_{eff} is used. The cases shown in the figure correspond to $\Delta E = 24$, $w = 4$ (Regime I) and $\Delta E = 12$, $w = 4$ (Regime II).

$$l_{eff} = \sigma l \quad (5)$$

where $\sigma = 1$ for chessboard topography, $\sigma = 2$ for random square patches and for ordered strips, and $\sigma = 4$ for random strips. These values of σ have been calculated analytically in ref 21. Figure 4 shows how simulation data for the function χ cast over a single curve for Regime I when the effective length scale is used. In general, it is found that χ obeys a power law in l_{eff} of the form

$$\ln \chi = \text{const} + \alpha \ln l_{eff} \quad (6)$$

This scaling behavior is found to hold over the whole range of energy, with different values of the exponent α given by

$$\alpha = \alpha_1 = -0.976 \pm 0.053 \quad \text{for } w/\Delta E \leq 1/4$$

$$\alpha = \alpha_2 + [12(1/3 - w/\Delta E)]^{\beta}(\alpha_1 - \alpha_2) \quad \text{for } 1/4 \leq w/\Delta E \leq 1/3 \quad (7)$$

$$\alpha = \alpha_2 = -1.525 \pm 0.065 \quad \text{for } w/\Delta E \geq 1/3$$

with $\beta = 0.42 \pm 0.04$. These results are similar to those obtained in previous works[19−22] with the difference that the value of the exponent α obtained previously is the double of the value given in eq 7 due to the difference in definition of the function χ.

It is to be noted that, in the case of attractive interactions, $w < 0$, only Regime I is possible and the value of exponent α is given by α_1 over the whole energy range.

As the temperature is changed, the scaling exponent does not change for Regime I, while for Regime II its value approaches that corresponding to Regime I, as temperature increases, in the form

$$\alpha_2(k_BT/\Delta E) = -1 - 0.806 \exp(-5.2174 k_BT/\Delta E) \quad (8)$$

Simulations have shown that this variation with temperature is also approximately valid in the intermediate range between Regimes I and II; therefore, eqs 7 and 8 give the general behavior of α over the whole energy range and for all temperatures. This behavior is shown in Figure 5.

Just as in previous works, it is found that the scaling exponent α presents *universality properties*, in the sense that its behavior

(24) Unfortunately, a typing error was included in the definition of the scaling function χ in refs 19−22, where the square of the integrated quantity was omitted.

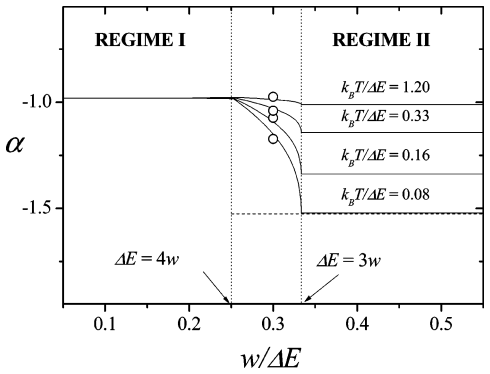

Figure 5. Behavior of the scaling exponent α over the whole range of energy.

and value are identical for different degrees of heterogeneity, ΔE, different topographies, different reference curves (even a theoretical reference curve like, for example, the mean field solution corresponding to bp) and for a definition of χ involving the function $q_d(\theta)$ instead of the function $\theta(\mu)$. It is therefore important to base the understanding of the observed behavior on an appropriate physical interpretation.

With this purpose, we start from the basic thermodynamic relationship[25]

$$\mu = \left(\frac{\partial F}{\partial N}\right)_{T,M} \tag{9}$$

where F is the Helmholtz free energy. Introducing the free energy per site, $f = F/M$, the last equation can be rewritten in terms of intensive variables in the form: $\mu = (\partial f/\partial\theta)_T$. Accordingly, the area to the left of each adsorption isotherm corresponding to a topography characterized by l in Figures 2 and 3 up to a determined coverage θ is given by

$$A(\theta,l) = \int_0^\theta \mu \, d\theta = f(\theta,l) - f(0,l) \tag{10}$$

Therefore, this area represents the variation in free energy per site in filling a surface, with topography characterized by the patch size l, up to a coverage θ.

Following this line of reasoning, and making use of the symmetry properties of the adsorption isotherm, which are a consequence of the vacancy-particle symmetry, the function χ, representing the area between a given isotherm and the bp reference isotherm, turns out to be

$$\chi(l) = 2[A(^1/_2,\text{bp}) - A(^1/_2,l)] \tag{11}$$

From eqs 10 and 11 we obtain

$$\chi(l) = 2[f(^1/_2,\text{bp}) - f(^1/_2,l)] \tag{12}$$

Therefore, the function χ defined in eq 4 is simply twice the difference in free energy per site between the reference isotherm (in this case that corresponding to bp) and the given isotherm, at half coverage. This result also explains why it depends on the topography parameter l: because the free energy at half coverage depends strongly on the structure of the adsorbate, which changes with l.

Calculation of the way in which this free energy changes with l leads to the physical significance and determination of the scaling exponent α. Without any loss of generality, we choose for this calculation the case of chessboard topography in Regime I. As already described in our discussion of the characteristics of Regime I, at half coverage strong site patches are completely filled while weak site patches are empty. Under these conditions, and considering that $f = u - Ts$, where u and s are the internal energy and configurational entropy per site, respectively, we obtain

$$f(^1/_2,\text{bp}) = u(^1/_2,\text{bp}) = (\epsilon_2 + 2w)/2 \tag{13}$$

$$f(^1/_2,l) = u(^1/_2,\text{bp}) = \epsilon_2/2 + w(l-1)/l \tag{14}$$

since $s(^1/_2,\text{bp}) = s(^1/_2,l) = 0$. By substituting eqs 13 and 14 in eq 12, we finally obtain

$$\chi(l) = 2w/l \tag{15}$$

which represents a power law with exponent $\alpha = -1$, as determined through simulations for Regime I. The same kind of analysis can be straightforwardly carried out for other topographies and for Regime II, leading to the values of the scaling exponent already determined by simulations. Of course, the value of α cannot be determined by these simple arguments in the intermediate regime (because of the problem of the determination of the configurational entropy for system of interacting particles), but the physical meaning of the scaling behavior is just the same.

The above analysis allows us also to understand the universality properties of the scaling exponent we described above. In particular, given that the function χ is related to the free energy per site at half coverage, and that the entropy per site is null at half coverage for both regimes (in fact for Regime II we have a unique ordered $c(2 \times 2)$ structure on both strong and weak patches), from the definition of the differential heat of adsorption, eq 3, we can easily see that the observed scaling behavior should also be valid for the function

$$\chi_q = \int_0^1 |q_d(\theta) - q_d^R(\theta)| \, d\theta \tag{16}$$

and this is verified through simulations.

In previous works it was shown how the scaling behavior could be used in the characterization problem, i.e., in obtaining information about the energetic topography from adsorption experiments of gases on heterogeneous surfaces. The present analysis provides fundamental physical insight into the scaling behavior and much more confidence for the proposed method based on the understanding of how the scaling works.

4. Conclusions

The scaling properties of adsorption of gases on heterogeneous surfaces characterized by a bivariate adsorption energy (strong and weak sites) and different kinds of patchwise topographies have been reviewed by using a different scaling function, χ, than that used in previous studies.

The present scaling function is shown to be directly related to the free energy per site of the adsorbed layer at half coverage. Taking advantage of the fact that the configurational entropy at half coverage is null, it is shown how the function χ scales as a power law with the effective length l_{eff} characterizing the energetic topography of the surface and how the scaling exponent α can be obtained. The analysis provides a physical understanding of the scaling behavior.

(25) Hill, T. L. *An Introduction to Statistical Thermodynamics*; Addison Wesley: New York, 1960.

The scaling behavior and the value of the scaling exponent α are determined over the whole range of interparticles interaction energy and adsorptive energy, and for different temperatures, through Monte Carlo simulations. The results are similar to those obtained in previous studies, with a value of α which is half the one obtained before due to the different definition of the scaling function, but the present analysis provides a full understanding of the scaling behavior based on the physical significance of the scaling function and the scaling exponent.

Acknowledgment. The Consejo Nacional de Investigaciones Científicas y Técnicas (CONICET) of Argentina is gratefully acknowledged for providing partial support of this research.

LA062491S